Prepared for submission to JHEP

Dark Gauge Bosons: LHC Signatures of Non-Abelian Kinetic Mixing

Carlos A. Argüelles,[a,b] **Xiao-Gang He,**[c,d,e] **Grigory Ovanesyan,**[f] **Tao Peng,**[a] **and Michael J. Ramsey-Musolf**[f,g]

[a] *Department of Physics, University of Wisconsin, Madison, WI 53706, USA*
[b] *Wisconsin IceCube Particle Astrophysics Center, Madison, WI 53703, USA*
[c] *INPAC, SKLPPC, and Department of Physics, Shanghai Jiao Tong University, Shanghai, China*
[d] *Physics Division, National Center for Theoretical Sciences, Department of Physics, National Tsing Hua University, Hsinchu 300, Taiwan*
[e] *CTS, CASTS, and Department of Physics, National Taiwan University, Taipei 106, Taiwan*
[f] *Amherst Center for Fundamental Interactions, Department of Physics, University of Massachusetts Amherst, Amherst, MA 01003, USA*
[g] *Kellogg Radiation Laboratory, California Institute of Technology, Pasadena, CA 91125, USA*

E-mail: arguelles@wisc.edu, hexg@phys.ntu.edu.tw, ovanesyan@umass.edu, mjrm@physics.umass.edu, tpeng23@wisc.edu

Abstract: We consider non-abelian kinetic mixing between the Standard Model $\mathrm{SU}(2)_L$ and a dark sector $\mathrm{U}(1)'$ gauge group associated with the presence of a scalar $\mathrm{SU}(2)_L$ triplet. The magnitude of the resulting dark photon coupling ϵ is determined by the ratio of the triplet vacuum expectation value, constrained to by $\lesssim 4$ GeV by electroweak precision tests, to the scale Λ of the effective theory. The corresponding effective operator Wilson coefficient can be $\mathcal{O}(1)$ while accommodating null results for dark photon searches, allowing for a distinctive LHC dark photon phenomenology. After outlining the possible LHC signatures, we illustrate by recasting current ATLAS dark photon results into the non-abelian mixing context.

arXiv:1604.00044v1 [hep-ph] 31 Mar 2016

Contents

1 Introduction **1**

2 The Model **4**

3 Collider phenomenology **5**
- 3.1 Production 6
- 3.2 Triplet-like scalar decay branching ratios 6
- 3.3 Various regimes for collider phenomenology 8

4 ATLAS recast **8**

5 Outlook **10**

A Feynman rules relevant for collider signatures **10**

1 Introduction

The search for weakly coupled light vector bosons has been a subject of considerable interest in recent years. Searches have been carried out in a number of different contexts, including low energy colliders, meson decays, beam dump experiments, and high-energy colliders (see, *e.g.*, Refs. [1, 2] and references therein). Theoretical studies typically assume that interactions of the "dark photon" with the visible sector are mediated by abelian kinetic mixing between the Standard Model (SM) hypercharge and the dark U(1)$'$ gauge groups [3–5]. For the "dark Z", mixing with the SM Z-boson may also occur *via* the mass terms in the Lagrangian[6, 7]. For both abelian and mass-mixing, the effects arise at the level of renormalizable operators. The resulting coupling of the dark vector bosons to the SM are then parameterized by a dimensionless parameter ϵ that is constrained by experiment to be $\lesssim 10^{-3}$ or smaller when for dark boson masses below ~ 10 GeV. The small scale of ϵ has no obvious origin in this context, so one must resort to models to explain why it is not $\mathcal{O}(1)$.

In this study, we observe that non-abelian kinetic mixing between the U(1)$'$ and the SM SU(2)$_L$ gauge groups, encoded in non-renormalizable operators, can provide a simple explanation without assuming tiny operator coefficients in the effective theory. Doing so requires augmenting the SM field content with additional bosons gauge bosons transforming non-trivially under SU(2)$_L$. For concreteness, we consider the scalar triplet[1] $\Sigma \sim (1, 3, 0, 0)$

[1] We list the quantum numbers in the order $SU(3)_{\rm C} \times SU(2)_{\rm L} \times U(1)_{\rm Y} \times G_{\rm D}$, where $G_{\rm D}$ is the dark gauge group.

and focus on the dimension-five operator

$$\mathcal{O}_{WX}^{(5)} = -\frac{\beta}{\Lambda} \mathrm{Tr}\left(W_{\mu\nu}\Sigma\right) X^{\mu\nu} \tag{1.1}$$

where $X^{\mu\nu}$ and $W^{\mu\nu}$ are the $\mathrm{U}(1)'$ and $\mathrm{SU}(2)_L$ field strength tensors, respectively; $\Sigma = \Sigma^a T^a$ with T^a being the $\mathrm{SU}(2)_L$ generators; and Λ is the mass scale associated with fields that have been integrated out in generating the operator. A non-zero vacuum expectation value $\langle \Sigma^0 \rangle \equiv v_\Sigma$ will lead to mixing between the $\mathrm{U}(1)'$ boson X_μ and the neutral $\mathrm{SU}(2)_L$ gauge boson W_μ^3. The mixing parameter is then given by

$$\epsilon = \beta \sin\theta_W \left(\frac{v_\Sigma}{\Lambda}\right) \quad , \tag{1.2}$$

where θ_W is the weak mixing angle. The scale ratio v_Σ/Λ the controls the magnitude of ϵ. Importantly, constraints from electroweak precision tests constrain the triplet vev to be relatively small: $v_\Sigma \lesssim 4$ GeV. Thus, ϵ will satisfy the experimental bounds for Λ larger than about one TeV for $\beta \sim \mathcal{O}(1)$.

The idea of non-abelian kinetic mixing is not original to us. The authors of Ref. [8] considered $\mathrm{U}(1)_Y \times \mathrm{SU}(2)'$, with the latter factor being a dark SU(2) gauge group. Dark SU(2) gauge invariance requires introduction of an additional scalar triplet $\Sigma_D \sim (1, 1, 0, 3)$, allowing for a dimension five mixing operator analogous to that of Eq. (1.1). In contrast to the present case, however, the dark triplet vev can have any magnitude, and for large values, a small ϵ requires a commensurately small operator coefficient. In a follow-up work [9] applications for astrophysical anomalies and other constraints are studied in this scenario. In Ref. [10] this non-abelian kinetic mixing is used to explain the X-ray line at 3.55 keV.

More recently, the authors of Ref. [11] considered $\mathrm{SU}(2)_L \times \mathrm{U}(1)'$ kinetic mixing *via* the dimension six operator

$$\frac{C}{\Lambda^2} H^\dagger T^a H W_{\mu\nu}^a X^{\mu\nu} \tag{1.3}$$

where H is the SM Higgs doublet, leading to $\epsilon \sim C(v/\Lambda)^2$. Assuming this operator arises at one-loop, one has $\Lambda \sim 4\pi m_\phi$, where m_ϕ is the mass of the mediator in the loop. For $\Lambda \gtrsim 10$ TeV (or $m_\phi \gtrsim 1$ TeV), one may satisfy the experimental constraints on ϵ for $C \sim \mathcal{O}(1)$. The authors of this work consider an explicit model with a scalar mediator $\phi \sim (1, 3, 0, q_D)$ and a dark Higgs $h_D \sim (1, 1, 0, q_D)$ that is responsible for generating the dark photon mass. A detailed analysis of the collider signatures associated with the dark bosons is given.

In what follows, we concentrate on the collider signatures associated with the dimension five operator (1.1) rather than on construction of an explicit dark sector mediator model. In particular, we note that final states containing one or more X bosons may be produced through two distinct mechanisms, each of which involves $\mathcal{O}_{WX}^{(5)}$ directly: (1) Drell-Yan pair production of Σ states, $pp \to V \to \Sigma\Sigma$, followed by the $\mathcal{O}_{WX}^{(5)}$-induced decay $\Sigma \to XV$, resulting in a $XXVV$ topology; (2) direct production *via* $\mathcal{O}_{WX}^{(5)}$, $pp \to V^* \to X\Sigma$, followed by the the decay $\Sigma \to XV$, generating a final state of the topology XXV. For sufficiently large β/Λ the direct production mechanism (2) may dominate. In this case, v_Σ must be

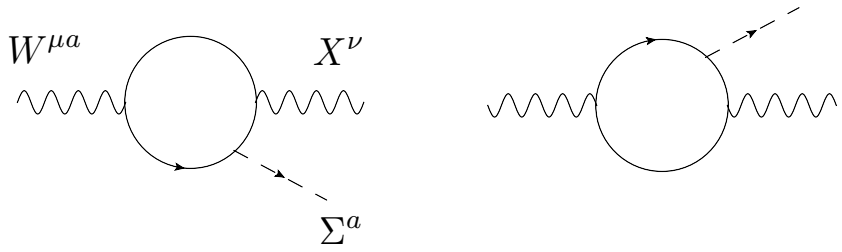

Figure 1. Feynman graphs that may generate non-abelian mixing $\mathrm{SU}(2)_L \times \mathrm{U}(1)'$. Here, the mediators in the loop may be either fermions or scalars.

sufficiently small to ensure the experimental constraints on ϵ are satisfied. Conversely, for smaller β/Λ (larger v_Σ for a given ϵ), production will occur primarily through the Drell-Yan process[2]. For similar reasons, the Σ-decay branching ratios will also carry a dependence on β/Λ (and, thus, on v_Σ for fixed ϵ). In what follows, we delineate several general parameter space regimes associated with this interplay of parameters.

For concrete illustration, we then consider the present LHC sensitivity for the regions of parameter space where the direct production mechanism dominates and where the $\Sigma \to VX$ branching ratio is close to unity. For this parameter space region and for $m_X > 2m_\mu$, one expects displaced vertices associated with $X \to \mu^+\mu^-$ decays, where the dimuon pair appears as a lepton jet. The ATLAS collaboration has performed a search for events of this type that involve two or four lepton jets[12]. We carry out a simple recast of the corresponding ATLAS bound on long-lived dark bosons for our scenario, noting that the ATLAS search is inclusive and accommodates additional, unobserved, final state SM gauge bosons. For dark boson mass m_X in the range $0.2\,\mathrm{GeV} \leq m_X \leq 2\,\mathrm{GeV}$ we find that the present ATLAS exclusion can extend to $\Lambda/\beta \sim$ several hundred GeV, depending on the value of v_Σ. We also discuss the possibilities for future collider tests of this scenario, including searches that would identify the SM final state gauge bosons.

Our discussion of this scenario and collider analysis is organized as follows. In Section 2 we review the setup of the triplet-assisted non-abelian kinetic mixing. In Section 3 we outline distinctive LHC signatures for our scenario and in Section 4 we present the recast of ATLAS bounds on dark photons for the non-abelian kinetic mixing. Finally, we conclude in Section 5.

2 The Model

We add to SM Lagrangian dimension four operators involving dark photon and the real triplet fields, as well as dimension five effective operators:

$$\mathcal{L} = \mathcal{L}_{\rm SM} + \Delta\mathcal{L}^{(d=4)} + \Delta\mathcal{L}^{(d=5)} + \dots \ . \tag{2.1}$$

The dimension four and five operators we take to be of the form:

$$\begin{aligned}
\Delta\mathcal{L}^{(d=4)} &= -\frac{1}{4}X_{\mu\nu}X^{\mu\nu} + \frac{\epsilon_0}{2\,c_W}B_{\mu\nu}X^{\mu\nu} + {\rm Tr}\left[(D_\mu\Sigma)^\dagger\, D_\mu\Sigma\right] - V(\Sigma,H) + \Delta\tilde{\mathcal{L}}^{(d=4)}, \\
\Delta\mathcal{L}^{(d=5)} &= -\frac{1}{\Lambda}\,{\rm Tr}\left(W_{\mu\nu}\Sigma\right)\left(\alpha B^{\mu\nu} + \beta X^{\mu\nu}\right) \equiv \mathcal{O}^{(5)}_{WB} + \mathcal{O}^{(5)}_{WX}\,.
\end{aligned} \tag{2.2}$$

Here, $\Delta\mathcal{L}^{(d=4)}$ contains the usual abelian (XB) kinetic mixing term and c_W is the cosine of the weak mixing angle. The terms breaking the dark $U(1)'$ gauge group are not explicitly presented and are part of $\Delta\tilde{\mathcal{L}}^{(d=4)}$. The real triplet field Σ and the scalar triplet-doublet potential are given by [13]:

$$\Sigma = \frac{1}{2}\begin{pmatrix} \Sigma^0 & \sqrt{2}\Sigma^+ \\ \sqrt{2}\Sigma^- & -\Sigma^0 \end{pmatrix}, \qquad D_\mu\Sigma = \partial_\mu\Sigma + ig\left[\sum_{a=1}^{3} W^a_\mu T^a, \Sigma\right], \tag{2.3}$$

$$V(H,\Sigma) = -\mu^2 H^\dagger H + \lambda_0\left(H^\dagger H\right)^2 - \mu_\Sigma^2\, G + b_4 G^2 + a_1\, H^\dagger\Sigma H + a_2 H^\dagger H G, \tag{2.4}$$

where $G \equiv {\rm Tr}\Sigma^\dagger\Sigma = \frac{\left(\Sigma^0\right)^2}{2} + \Sigma^+\Sigma^-$. In the notation of Ref. [13], $G = F/2$.

Given a UV complete theory one may integrate out heavy states that have both SM and dark charges, as illustrated in Figure 1. We leave the model-dependent details of the full theory unspecified, focusing instead on $\mathcal{O}^{(5)}_{WX}$ and the corresponding collider phenomenology. In addition it is possible that similar graphs as in Figure 1 generate the effective dimension five operator $\mathcal{O}^{(5)}_{WB}$. After electroweak symmetry breaking (EWSB), this operator will contribute to the S parameter:

$$\alpha_{\rm em} S = 4 c_W s_W \frac{\alpha v_\Sigma}{\Lambda}. \tag{2.5}$$

This sets a 90% CL bound $\alpha v_\Sigma/\Lambda \lesssim 0.0008$. We will henceforth set $\alpha = 0$ and concentrate on the phenomenology associated with $\mathcal{O}^{(5)}_{WX}$.

Before proceeding, we comment here that kinetic mixing of gauge bosons can also be realized for non-abelian groups. For example, for a SU(N)×SU(M) gauge theory with gauge fields W and Y, one can introduce a scalar field Δ^{ab} transforming as the adjoint representation under both the SU(N)×SU(M) groups, with indices "a" and "b" corresponding to

[2] In principle, the same set of possibilities applies to the operator (1.3); in practice, they are less likely to be realized, since the minimum value of Λ is roughly ten times larger than for the interaction (1.1) and since the dimension six operator carries a quadratic dependence on the inverse mass scale. Thus, consideration of the dark sector mediators responsible for (1.3) as analyzed in Ref. [11] may be the most promising probe in the latter case.

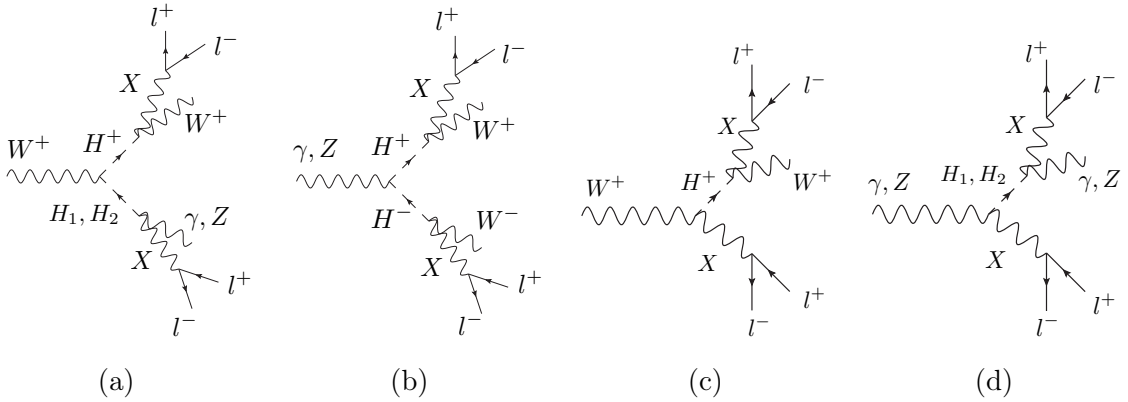

Figure 2. Feynman graphs for LHC production and decay of the particles in the triplet-assisted non-abelian mixing model. Diagrams (a,b) indicate scalar pair production, followed by $\mathcal{O}^{(5)}_{WX}$-mediaed scalar decays. Diagrams (c,d) inducate $\mathcal{O}^{(5)}_{WX}$-mediated production and decays. In all graphs, the incoming vector boson is virtual.

SU(N) and SU(M), respectively. In analogy with $\mathcal{O}^{(5)}_{WX}$, one can construct the $d = 5$ operator $W^{a\mu\nu}Y^b_{\mu\nu}\Delta^{ab}$. A non-vanishing vev for Δ^{ab} will lead to kinetic mixing between W and Y. One may also construct renormalizable models that generate this operator at the one-loop level. We defer a detailed consideration of this possibility to a future study.

3 Collider phenomenology

In the presence of $\mathcal{O}^{(5)}_{WX}$, the collider phenomenology associated with the real triplet can differ substantially from what has been considered previously in Ref. [13]. To illustrate the key features, we will make the following assumptions:

(a) The potential parameters are chosen so as to render the doublet-triplet mixing angle – proportional to v_Σ – to be small, but non-vanishing. In this case the neutral scalar sector will consist of two states, $H_{1,2}$, with H_1 being primarily the SM Higgs boson and H_2 being primarily Σ^0. In the charged scalar sector, doublet-triplet mixing implies that the physical charged triplet states $H^\pm$ are not pure triplet states, but rather mixtures of $\Sigma^\pm$ and the charged components of the doublet, with the the other combination providing the longitudinal components of the massive weak gauge bosons. Note that in the absence of doublet-triplet mixing, $\mathrm{SU}(2)_L\times\mathrm{U}(1)_Y$ gauge invariance precludes Σ from coupling to the SM fermions. The presence of a non-vanishing mixing angle then introduces a coupling of $H^\pm$, H_2 to the SM fermions through the SM Yukawa interactions.

(b) For $v_\Sigma = 0$, the triplet states have a common mass, give by $m^2_\Sigma = -\mu^2_\Sigma + a_2v^2/2$. Electroweak loops raise the mass of the charged components with respect to that of the neutral component by ~ 166 MeV, allowing for the decay $H^+ \to H_2\pi^+$. Our choice of the potential parameters will not substantially alter this splitting even for $v_\Sigma \neq 0$.

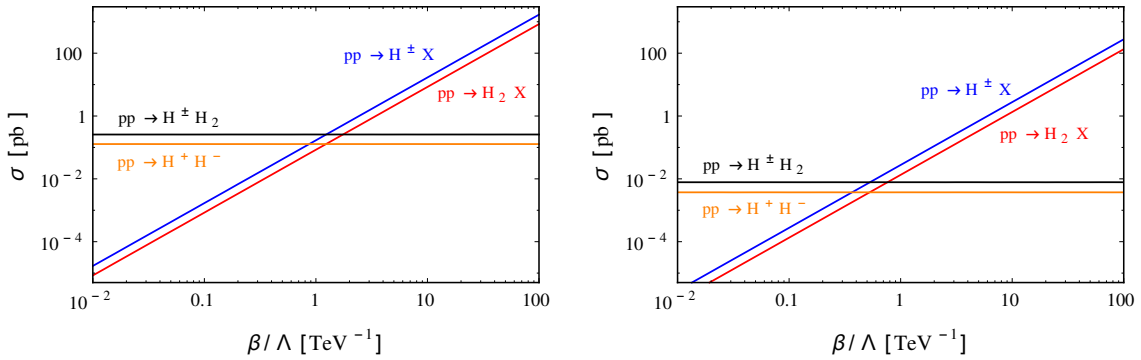

Figure 3. Production cross sections for $pp \to V \to \phi\phi$ and $pp \to V \to X\phi$ for associated triplet-like states $\phi = H^+, H_2$ and a dark photon X with mass $m_X = 0.4$ GeV. For the final states containing a single charged scalar and one neutral boson, we have summed the cross sections for both charges [*e.g.* $\sigma(H^+H_2) + \sigma(H^-H_2)$]. The left and right panels correspond to $m_\phi = 130$ GeV and $m_\phi = 300$ GeV, respectively.

With these comments in mind, we now consider the production and decays of the triplet-like scalars.

3.1 Production

The LHC production and decay mechanisms of interest are shown in Figure 2. Graphs (a) and (b) indicate Drell-Yan pair production, $pp \to V^* \to \phi\phi$, where ϕ denotes any of the physical scalars, with the subsequent decays $\phi \to XV$, leading to the topology $XXVV$. As discussed above, the ϕ states will be predominantly triplet-like. Graphs (c) and (d) show the $\mathcal{O}^{(5)}_{WX}$-mediated production $pp \to V^* \to \phi X$, with a subsequent decay $\phi \to XV$, leading to the topology XXV. (Feynman rules for the vertices in Figure 2 are listed in the Appendix A.)

In Figure 3 we show the the LHC production cross sections for different channels at $\sqrt{s} = 8$ TeV . The left panel corresponds to $m_\phi = 130\,\text{GeV}$ and the right one corresponds to $m_\phi = 300\,\text{GeV}$. For both masses we observe that for $\beta/\Lambda \lesssim 1\,/\,\text{TeV}$ the Drell-Yan pair production dominates, while for $\beta/\Lambda \gtrsim 1\,/\,\text{TeV}$ $\mathcal{O}^{(5)}_{WX}$-mediated production is the dominant mechanism. For $\sqrt{s} = 14$ TeV the corresponding transition between Drell-Yan and $\mathcal{O}^{(5)}_{WX}$-mediated production occurs for approximately the same value of β/Λ.

3.2 Triplet-like scalar decay branching ratios

The triplet-like scalars $H^\pm$ and H_2 will decay to $W^\pm X$ and $Z/\gamma\, X$ respectively as well as to other final states as considered in Ref.[13]. For illustrative purposes we show the decay width for $H^\pm \to W^\pm X$, which is sufficient for the analysis that we consider below. The tree level $H^\pm \to W^\pm X$ decay rate is given by

$$\Gamma(H^\pm \to W^\pm X) \tag{3.1}$$

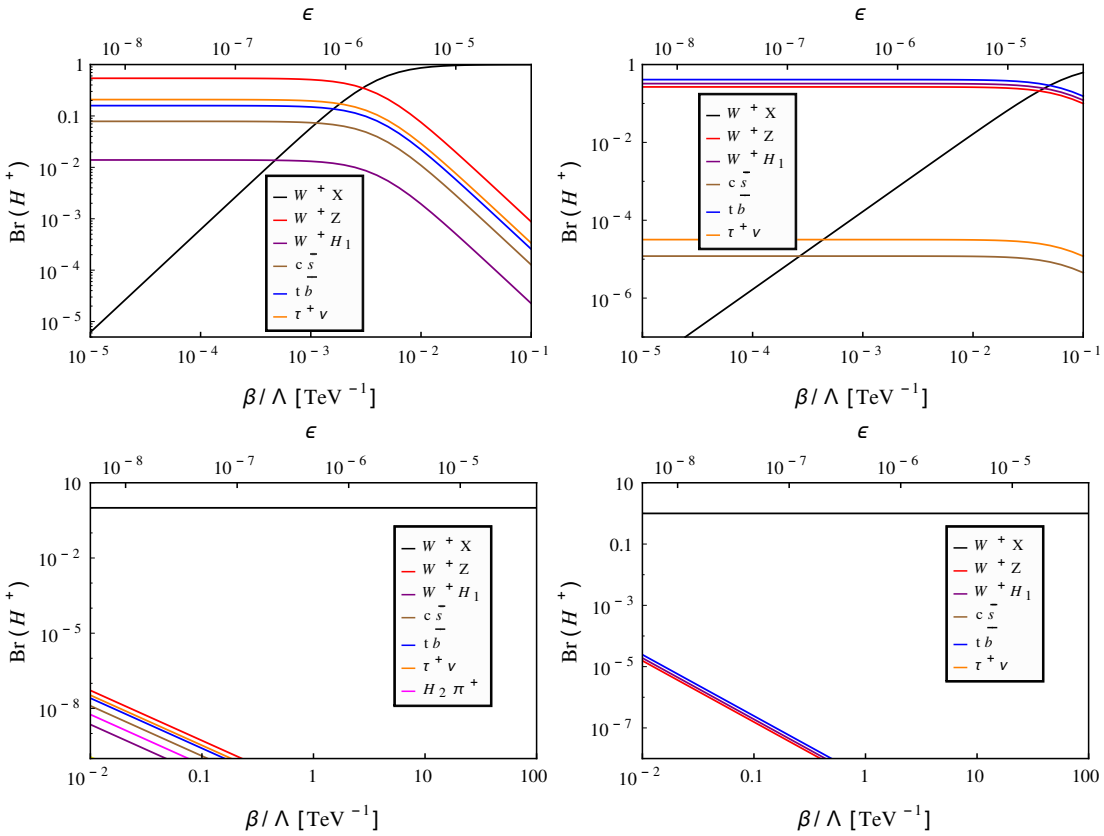

Figure 4. Branching ratios for H^+ decays as a function of β/Λ (bottom horizontal axis) and ϵ (upper horizontal axis) for $m_X = 0.4$ GeV. The top (bottom) row corresponds to $v_\Sigma = 1$ GeV ($v_\Sigma = 10^{-3}$ GeV), while the left (right) column corresponds to $m_{H^+} = 130$ GeV ($m_{H^+} = 130$ GeV). The solid black line indicates the branching ratio for $H^+ \to W^+X$. Branching ratios for other final states are as indicated by the legend insert.

$$= \frac{\sqrt{1 - \frac{2(m_X^2+M_{W^\pm}^2)}{M_{H^\pm}^2} + \frac{(m_X^2-M_{W^\pm}^2)^2}{M_{H^\pm}^4}}}{16\pi M_{H^+}} \left[\frac{1}{2}\left(M_{H^\pm}^2 - m_X^2 - M_{W^\pm}^2\right)^2 + M_X^2 M_{W^\pm}^2\right] \frac{\beta^2}{\Lambda^2} c_\mp^2 \,,$$

where $c_\mp$ is the mixing angle associated with diagonalizing the charged scalar sector. Combined with the other H^+ decay channels [13] we compute the branching ratios shown in Figure 4. The left and right panels correspond to $m_{H^+} = 130\,\text{GeV}$ and $m_{H^+} = 300\,\text{GeV}$, respectively. The top panels correspond to $v_\Sigma = 1\,\text{GeV}$ and the bottom ones to $v_\Sigma = 1\,\text{MeV}$.

From the plots in Figure 4 we see that for $v_\Sigma = 1\,\text{GeV}$, a value near the maximum allowed by electroweak precision tests, the branching ratio for $H^+ \to W^+X$ is essentially 100% when $\epsilon \gtrsim 10^{-4}$. For the smaller value of $v_\Sigma = 1\,\text{MeV}$, the branching ratio is essentially 100% for all values of ϵ. This translates into the range $\beta/\Lambda \gtrsim 0.1/\text{TeV}$ for the branching ratio to be essentially 100% independent on the value of the vev. For lower values of β/Λ any branching ratio from zero to one is possible, and the precise value depends strongly on the value v_Σ.

3.3 Various regimes for collider phenomenology

From the forgoing discussion of production and decays, the LHC signatures and detection strategies will vary according to the value of β/Λ. We delineate three regimes leading to distinctive phenomenology for 8 TeV pp center of mass energy:

(1) $\beta/\Lambda \lesssim 1/\text{TeV}$. In this regime we see that Drell-Yan pair production $p \to \phi\phi$ dominates In addition the branching ratio for $\phi \to XV$ decay is close to hundred percent.

(2) $1/\text{TeV} \lesssim \beta/\Lambda \lesssim 10^{-3}/\text{TeV}$. In this regime Drell-Yan pair production remains the dominant mechanism. However, $\text{BR}(\phi \to XV)$ can range from zero to one, depending on value of v_Σ.

(3) $\beta/\Lambda \gtrsim 1/\text{TeV}$. In this regime the $\mathcal{O}^{(5)}_{WX}$-mediated process $pp \to X\phi$ is dominant $\text{BR}(\phi \to XV)$ is close to one. In this case, the possible final states are indicated in Figure 2(c,d).

(Recall that for $\sqrt{s} = 14$ TeV, the transition between $\mathcal{O}^{(5)}_{WX}$-mediated production and Drell-Yan pair production also occurs for $\beta/\Lambda \sim 1/\text{TeV}$.) While all three possibilities above are worth exploration in future, for illustrative purposes we focus here on the third regime.

4 ATLAS recast

Considering now regime (3), we recast the ATLAS dark photon search results [12] into constraints on our scenario. The analysis of Ref. [12] assumes the presence of a SM Higgs boson decaying to two new states that radiate two (or four) dark photons, leading to displaced vertices and lepton jets. This is to be compared to our production scenario mediated by an off-shell vector boson V^*, leading to a final state containing two X bosons and an on-shell V. Note, that the ATLAS study [12] only applied cuts to isolate events with lepton jets and displaced vertices. No reconstruction of the Higgs boson invariant mass was preformed, nor were cuts on the missing energy applied. Thus, although the ATLAS study was carried out assuming different underlying X-boson production dynamics, the analysis is sufficiently inclusive to accommodate the scenario considered here as well. Looking to the future, we note that one could likely improve the LHC sensitivity to $\mathcal{O}^{(5)}_{WX}$ by including additional criterial need to identify the final state V.

We then translate the ATLAS bounds on $\epsilon - m_X$ parameter space[12] to the parameter space relevant to our scenario. Certain distinctions between the analysis of Ref. [12] and that for our scenario have to be accounted for properly. Specifically, Ref. [12] presents the 95% C.L. exclusion plots for the signal cross section $\sigma(H) \times \text{Br}(H \to 2X + \cdots)$ as a function of the dark photon lifetime $c\tau$ (see the left panel of Figure 16 in that work[3]). In our case, the 95% C.L. bound applies to $\sigma(\phi X) \times \text{Br}(\phi \to VX)$. In addition, $\sigma(H)$ and $\text{Br}(H \to 2X + \cdots)$ are independent of ϵ (the dependence on m_X is negligible for very light dark bosons). The production cross section and branching ratios for our scenario,

[3]This bound is obtained by excluding from the analysis TYPE2-TYPE2 events, which correspond to both dark photons decaying to jets. This leads to a stronger bound due to corresponding backgrounds.

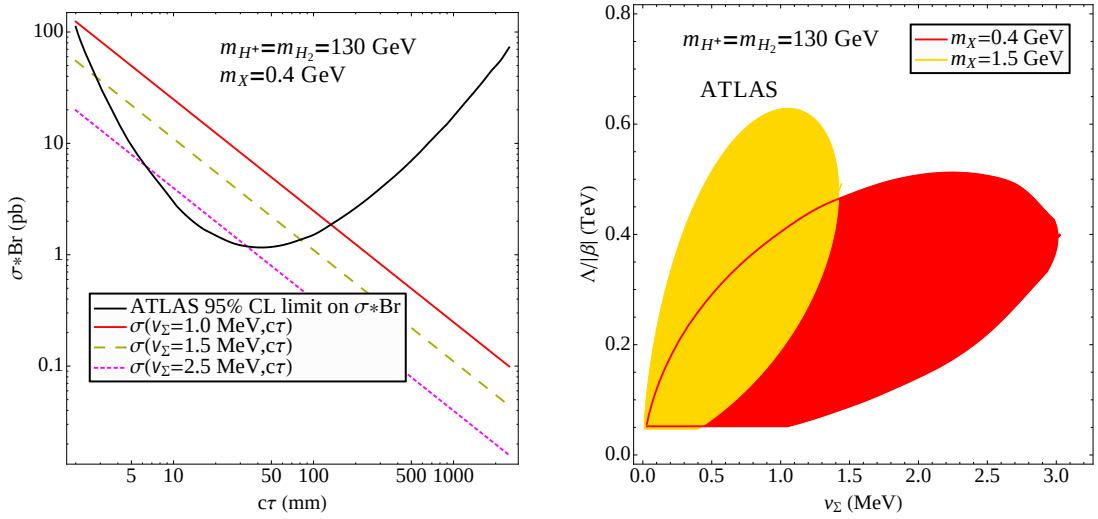

Figure 5. Constrains on triplet-assisted non-abelian kinetic mixing, recast from the ATLAS search reported Ref. [12]. The left panel gives the exclusion in the ($c\tau$, $\sigma \times$ BR) plane, where the region above the parabola is excluded. The diagonal lines indicate the dependence of $\sigma \times$ BR on $c\tau$ for different representative choices of v_Σ. The right panel gives the exclusion region in the(v_Σ, Λ/β) plane for $m_X = 0.4$ GeV (red region) and $m_X = 1.5$ GeV (yellow region).

on the other hand, depend on various combinations of the parameters that govern ϵ, *viz*, $\sigma(HX) \sim (\beta/\Lambda)^2 \sim 1/(\tau v_\Sigma^2)$, where τ is the X lifetime. In making the translation from Ref. [12] we then use the relation in Eq. (1.2).

In the left panel of Figure 5 we show the ATLAS 95% CL limit on $\sigma(\phi X)\times\mathrm{Br}(\phi \to VX)$, summing over all ϕ, for $m_X = 0.4\,\mathrm{GeV}$ (solid black) and lines of constant cross section $\sigma(pp \to \phi X)$ (again, summed over all ϕ) for three representative values of v_Σ: $v_\Sigma = 1\,\mathrm{MeV}$ (solid red), $v_\Sigma = 1.5\,\mathrm{MeV}$ (dashed olive) and $v_\Sigma = 2.5\,\mathrm{MeV}$ (dotted magenta). In each case, $\mathrm{Br}\,(\phi \to VX) \approx 100\%$. For each line of constant v_Σ the points of intersection with the solid black curve determine the boundaries of the region of excluded $c\tau$. We observe that the ATLAS exclusion then applies to v_Σ in the MeV range, well below the ρ-parameter bound. These results, together with Eq. (1.2), lead to constraints in the (v_Σ, β/Λ) plane, shown in the right panel of Fig. 5. For illustration we consider this translation for two values of m_X: 0.4 GeV (red) and 1.5 GeV (gold). We observe that the exclusion can reach Λ/β up to several hundred GeV, depending on the value of m_X and v_Σ. Note that for fixed Λ/β (fixed $\sigma \times$ BR) , $c\tau$ (ϵ) increases (decreases) with decreasing v_Σ. Thus, for a given Λ/β and sufficiently small v_Σ (equivalently ϵ), τ will fall below the ATLAS exclusion curve in the left panel of Fig. 5; hence, the exclusion limits on Λ/β in the right panel weaken with decreasing v_Σ.

5 Outlook

Mixing between the dark U(1)$'$ and SU(2)$_L$ gauge groups, mediated by the operator $\mathcal{O}^{(5)}_{WX}$, leads to a small mixing parameter ϵ, whose magnitude is set by the scale ratio v_Σ/Λ with an $\mathcal{O}(1)$ Wilson coefficient, β. The resulting collider phenomenology is quite distinctive, as $\mathcal{O}^{(5)}_{WX}$ may dominate the production of final states containing X bosons when $\Lambda/\beta \lesssim 1$ TeV at both $\sqrt{s} = 8$ TeV and $\sqrt{s} = 14$ TeV . Current ATLAS bounds, based on an inclusive search for pairs of lepton jets associated with displaced vertices, exclude Λ/β up to about 600 GeV, depending on the value of m_X and the triplet vev v_Σ. Looking to the future, the collection of additional data during Run II will extend the reach of the inclusive search. In the advent of a discovery, inclusion of additional search criteria associated with the final state vector boson(s) would allow one to distinguish this scenario from those associated with abelian kinetic mixing. An analysis of this possibility, along with the LHC sensitivity to other regions of the (m_X, ϵ) plane, will appear in future work.

Acknowledgments

We thank Jiang-Hao Yu and Jesse Thaler for useful discussions. This work was supported in part by U.S. Department of Energy contract DE-SC0011095 (G.O., T.P., and M.J.R.-M.). X-G He was supported in part by the MOE Academic Excellent Program (Grant No. 102R891505) and MOST of R.O.C. (Grant No. MOST104-2112-M-002-015-MY3), and in part by NSFC (Grant Nos. 11175115 and 11575111) and Shanghai Science and Technology Commission (Grant No. 11DZ2260700) of P.R.C. X. G. He also thanks Korea Institute for Advanced Study (KIAS) for their hospitality during the completion of this work.

A Feynman rules relevant for collider signatures

Feynman rules of interactions between the dark bosons, leptons, gauge bosons, charged and neutral Higgs bosons are listed in the table below:

Interaction	Feynman rule
Xl^+l^-	$ie\left(\epsilon_0 - \frac{\beta v_\Delta s_W}{\Lambda}\right)$
$W^\pm H^\mp X$	$\frac{i\beta}{\Lambda}\left(g^{\mu\nu}pp' - p^\nu p'^\mu\right) c_\mp$
ZH_1X	$\frac{i\beta}{\Lambda}\left(g^{\mu\nu}pp' - p^\nu p'^\mu\right) c_W s_0$
ZH_2X	$\frac{i\beta}{\Lambda}\left(g^{\mu\nu}pp' - p^\nu p'^\mu\right) c_W c_0$
AH_1X	$\frac{i\beta}{\Lambda}\left(g^{\mu\nu}pp' - p^\nu p'^\mu\right) s_W s_0$
AH_2X	$\frac{i\beta}{\Lambda}\left(g^{\mu\nu}pp' - p^\nu p'^\mu\right) s_W c_0$
$W^+_\mu(p_1)W^-_\nu(p_2)H_1X_\alpha(p_3)$	$\frac{i\beta g}{\Lambda}\left(p_3^\mu g^{\nu\alpha} - p_3^\nu g^{\mu\alpha}\right) s_0$
$W^+_\mu(p_1)W^-_\nu(p_2)H_2X_\alpha(p_3)$	$\frac{i\beta g}{\Lambda}\left(p_3^\mu g^{\nu\alpha} - p_3^\nu g^{\mu\alpha}\right) c_0$
$W^\pm_\mu(p_1)Z_\nu(p_2)\,H^\mp X_\alpha(p_3)$	$\mp\frac{i\beta g}{\Lambda}\left(p_3^\mu g^{\nu\alpha} - p_3^\nu g^{\mu\alpha}\right) c_W\, c_\mp$
$W^\pm_\mu(p_1)A_\nu(p_2)\,H^\mp X_\alpha(p_3)$	$\mp\frac{i\beta g}{\Lambda}\left(p_3^\mu g^{\nu\alpha} - p_3^\nu g^{\mu\alpha}\right) s_W\, c_\mp$

Feynman rules entering in the vertices of the graphs in Figure 2. Where $c_\mp \equiv \cos\theta_\mp$ and $c_0 \equiv \cos\theta_0$ are as defined in Ref. [13].

References

[1] R. Essig *et al.*, Working Group Report: New Light Weakly Coupled Particles, in *Community Summer Study 2013: Snowmass on the Mississippi (CSS2013) Minneapolis, MN, USA, July 29-August 6, 2013*, 2013, 1311.0029.

[2] D. Curtin, R. Essig, S. Gori, and J. Shelton, JHEP **02**, 157 (2015), 1412.0018.

[3] B. Holdom, Phys.Lett. **B166**, 196 (1986).

[4] R. Foot and X.-G. He, Phys.Lett. **B267**, 509 (1991).

[5] P. Fayet, Phys.Rev. **D70**, 023514 (2004), hep-ph/0403226.

[6] H. Davoudiasl, H.-S. Lee, and W. J. Marciano, Phys.Rev. **D85**, 115019 (2012), 1203.2947.

[7] H. Davoudiasl, H.-S. Lee, and W. J. Marciano, Phys.Rev. **D89**, 095006 (2014), 1402.3620.

[8] F. Chen, J. M. Cline, and A. R. Frey, Phys.Rev. **D79**, 063530 (2009), 0901.4327.

[9] F. Chen, J. M. Cline, and A. R. Frey, Phys.Rev. **D80**, 083516 (2009), 0907.4746.

[10] J. M. Cline and A. R. Frey, (2014), 1408.0233.

[11] G. Barello, S. Chang, and C. A. Newby, (2015), 1511.02865.

[12] ATLAS, G. Aad *et al.*, JHEP **11**, 088 (2014), 1409.0746.

[13] P. Fileviez Perez, H. H. Patel, M. Ramsey-Musolf, and K. Wang, Phys.Rev. **D79**, 055024 (2009), 0811.3957.